Phosphine Ligand-Free Bimetallic Ni(0)Pd(0) Nanoparticles as Catalyst for Facile, General, Sustainable, and Highly Selective 1,4-Reductions in Aqueous Micelles

*Deborah Ogulu,[†‡] Pranjal P. Bora,[†‡] Manisha Bihani,[†] Sudripet Sharma,[†] Tharique N. Ansari,[†] Andrew J. Wilson,[†] Jacek B. Jasinski,[§] Fabrice Gallou,[∥] Sachin Handa[†]**

[†]2320 S. Brook Street, Department of Chemistry, University of Louisville, Louisville, Kentucky 40292, United States

[§]Materials Characterization, Conn Center for Renewable Energy Research, University of Louisville, Louisville, Kentucky 40292, United States

[∥]Novartis Pharma AG, Basel, 4056, Switzerland

ABSTRACT. Phosphine ligand-free bimetallic nanoparticles (NPs) composed of Ni(0)Pd(0) catalyze highly selective 1,4-reductions of enones, enamides, enenitiles, and ketoamides under aqueous micellar conditions. A minimal amount of Pd (Ni:Pd = 25:1) is needed to prepare these NPs, which effect reductions without impacting *N*-and *O*-benzyl, aldehyde, nitrile, and nitro functional groups. A broad range of substrates has been studied, including a gram-scale reaction. The metal-micelle binding is supported by surface-enhanced Raman spectroscopy (SERS) data on both the NPs and their individual components. Optical imaging, high-resolution transmission

electron microscopy (HRTEM), and energy-dispersive X-ray spectroscopy (EDX) analyses reveal the formation of NP-containing micelles or vesicles, NP morphology, particle size distribution, and chemical composition, respectively. X-ray photoelectron spectroscopy (XPS) measurements indicate the oxidation state of each metal within these bimetallic NPs.

KEYWORDS. Micellar Catalysis • Nanoparticle Catalysis • Chemistry in Water • Amphiphile • Metal-Micelle synergy

Introduction.

Transition-metal catalysis entailing either a metal-hydride, hydrogen gas, or hydrogen spillover is extremely useful in 21st-century organic synthesis.[1-6] Among transition metals, nickel (Ni) and palladium (Pd) catalysts are well known for olefin[5-7] and nitro group reductions,[8-10] hydrogenolysis of *N*/*O*-benzyl[11] and benzyl carbamates,[12,13] and hydrodehalogenation,[14,15] etc.[16-20] Commercially available catalysts, such as Raney Ni and Pd/C, are primarily used for hydrogenation chemistry in industrial and academic labs.[21] However, both catalysts are often non-selective and require flammable organic solvents in the presence of hydrogen gas.[2] Therefore, their usage requires extreme safety precautions. Selective catalytic 1,4-reduction in the presence of *N*/*O*-benzyl and nitro groups can be challenging, and are typically run in a non-aqueous reaction medium—benzyl deprotection and nitro group reductions are simultaneously operative pathways in an aqueous reaction medium. Zhan and co-workers have reported selective chalcone reduction; however, a catalyst system requires polymeric phosphine ligand, the synthesis of which involves toxic DMF.[5] Moreover, the catalysis is non-selective in the presence of a nitro group,[5] while a high Pd(0) loading is required for use in a chlorinated solvent.[6] Therefore, a process that involves selective

catalysis and relies on a low Pd loading that can be run safely in an aqueous medium is highly desirable.[22]

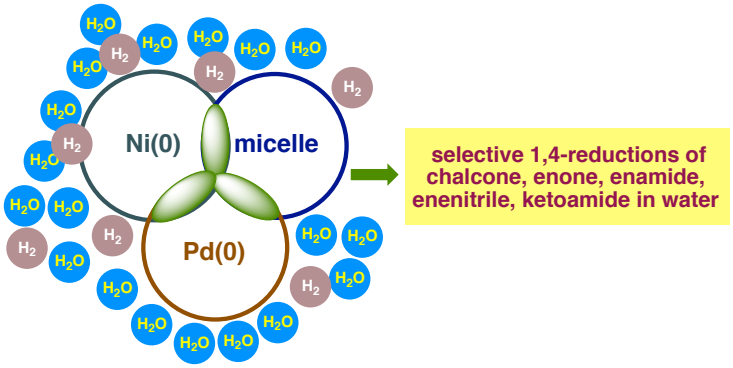

Figure 1. 1,4-reductions in water by bimetallic nanoparticles of Ni(0)Pd(0).

Bimetallic nanoparticles (NPs) containing Ni(0)Pd(0) that derive enhanced stability in an aqueous micellar medium should be available to facilitate catalysis in water.[12] Catalyst selectivity of these NPs is anticipated due to (a) a change in the NP surface free energy,[12,23,24] (b) modulation of surface properties arising from the binding of a NP-micelle in an aqueous environment, (c) availability of catalytic sites in the micellar interior, and (d) high solubility of hydrogen gas in the aqueous micellar medium (Figure 1).[12] The catalytic efficiency arising from NP-micelle synergy should also assist in reducing the loading of precious metals. The presence of the shielding effect of micelles could also play an important role in catalyst efficiency. This arises from binding between amphiphilic molecules of the micelle with the metal NP surface at either the micellar interface or its interior.[12] Likewise, these interactions controls the dynamic nature of the micelle, the NP morphology, surface area, and hence, overall catalytic activity. Therefore, to achieve these properties, careful selection of the amphiphile is necessary, as it must bind with the metal surface based on functionality contained within, and/or at the interface as NP are being formed, leading to uniform NP morphology and size. Such an amphiphile-catalyst association obviates the need for traditional phosphine ligands and yet, enables chemistry in water to take place.

Experimental

In a flame-dried 10 mL microwave reaction vial containing a PTFE-coated stir bar, $Ni(OAc)_2$ (44.5 mg, 0.25 mmol) was added under argon atmosphere. $Pd(OAc)_2$ (2.24 mg, 0.01 mmol) and 2.5 mL anhydrous THF was added to the reaction mixture under argon atmosphere. The reaction mixture was heated at 60 °C for 5 minutes and then the mixture was allowed to cool to rt. 3.0 M MeMgBr solution in diethyl ether (0.33 mL, 1 mmol) was added to the reaction mixture. Upon addition of Grignard reagent, the mixture turned to black color. The reaction mixture was stirred for 10 minutes at rt. 7.5 mL of 3.0 wt. % aq. PS-750-M was added to the reaction mixture and mixture was stirred at rt. After 20 minutes, THF was removed under reduced pressure. The reaction mixture was then centrifuged, and water layer was removed and dried under high vacuum overnight to obtain solid nanoparticles (for more details, see Supporting Information).

Results and Discussion

Since our amphiphile PS-750-M has an appropriate architecture that assists micelle-NP binding via its proline linker, our investigation began with the synthesis of bimetallic ligand-free NPs of Ni(0)/Pd(0) by combining $Ni(OAc)_2$ and $Pd(OAc)_2$ in a 25:1 ratio in THF. This mixture was then treated with MeMgBr leading to fast reduction and rapid nucleation and capping of the resulting NPs by addition of PS-750-M (for details, see Supporting Information, page S3). The *in-situ* formed NPs were then tested for activity towards 1,4-reduction of enone **1** in water using hydrogen as reductant. Clean conversion to **2** was obtained without the cleavage of the *O*-benzyl group, which is normally sensitive to such reduction conditions (Table 1, entry 1). Without prior formation of NPs, only 79% GC-MS conversion to the corresponding reduced product was obtained, which also contains 22% complex byproduct (entry 2). Removing Ni from the NPs

afforded only 77% GC-MS conversion to **2**, which also contains 17% byproduct (entry 3). Thus, NPs containing of both Ni((0) and Pd(0) afford a cleaner and more selective catalyst, leading to full conversion and a 94% isolated yield.

Table 1. Nanoparticle synthesis and catalytic reaction optimization

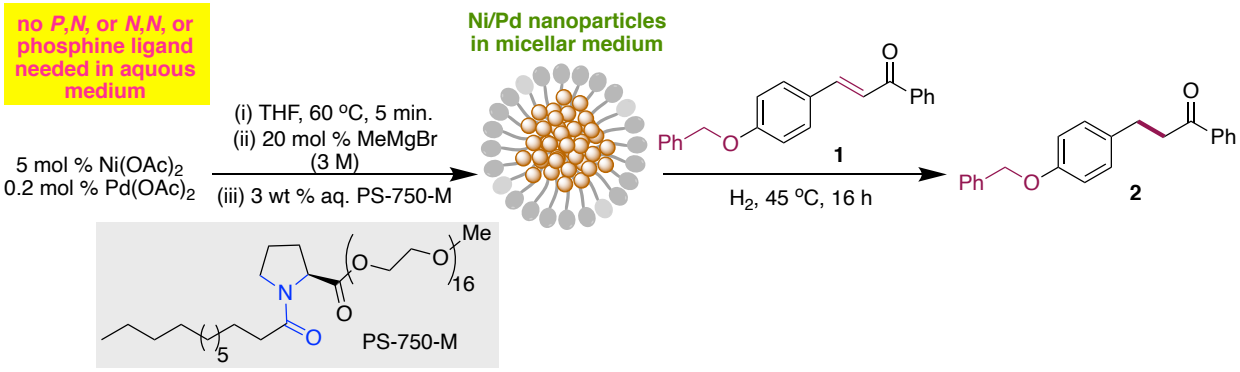

entry	deviations from standard conditions[a]	**2** (%)[b]
1	none	>99 (94)[c]
2	5 mol % $Ni(OAc)_2$, 0.2 mol % $Pd(OAc)_2$ instead of NPs	79[d]
3	No Ni in NPs, only Pd	77[e]
4	0.1 mol % Pd instead of 0.2 mol %	88
5	Ni NPs instead of Ni/Pd	traces
6	3 mol % Ni instead of 5 mol %	52
7	3 wt % proline instead of PS-750-M	traces
8	solvent THF instead of PS-750-M	NR
9	35 °C instead of 45 °C	63
10	$NaBH_4$ instead of H_2	64
11	0.5 M global conc. instead 0.25 M	82

[a]**Conditions**: $Ni(OAc)_2$ (2.2 mg, 0.0125 mmol, 5 mol %), $Pd(OAc)_2$ (0.11 mg, 0.0005 mmol, 0.2 mol %), 3.0 M MeMgBr solution in Et_2O (17 μL, 0.05 mmol, 20 mol %), 0.75 mL 3 wt % aq. PS-750-M, 0.25 mL THF, 0.25 mmol **1**, H_2 balloon; [b]GC-MS analysis; conversion based on unreacted starting material. [c]Isolated yield. NR = no reaction. [d]Product contains 22% unknown byproduct. [e]Product contains 17% unknown byproduct.

Altering the NP catalyst's Ni/Pd ratio to 50:1 lowered the extent of conversion to 88% under otherwise identical conditions (entry 4). However, the selectivity remained the same, i.e., no debenzylation and ketone reduction were observed. Removing the Pd from the NP catalyst led to only trace conversion to the desired product, leaving the unconsumed starting material. This indicates the importance of Pd in the NP catalyst (entry 5). The amount of Ni (5 mol %) was also found to be important. Reducing the Ni loading to 3 mol % results in only 52% conversion to the desired product (entry 6). Most notably, the reaction in water containing proline gives only traces of **2** (entry 7), indicative of the crucial role of the PS-750-M architecture as alluded to above. THF as an additive was necessary as **1** was insoluble in aqueous PS-750-M. However, no reaction was observed in neat THF solvent (entry 8). A reaction temperature of 45 °C was optimal; only 63% conversion was observed by GC-MS analysis when the reaction was conducted at 35 °C (entry 9). Hydrogen gas was found to be a more effective reductant compared to $NaBH_4$ (entry 10). A global concentration of 0.25 M was more effective than 0.5 M, perhaps minimizing opportunities for NP aggregation that decreases activity (entry 11).

Using the optimized reaction conditions, the substrate scope was next explored (Table 2, **2**-**17**). Most notably, reactions were clean and selective; with good-to-excellent isolated yields being obtained. A variety of *N*- and *O*-benzyl groups remained intact under the optimized reaction conditions. No debenzylation was observed in any example. Functional groups, such as trifluoromethyl (**4**), nitrile (**5**), ester (**6**), fluoro (**9**, **13**, **17**), acetyl (**13**), sulfonamide (**14**), amide (**15**), and aldehyde (**17**), were well tolerated. No nitrile reduction or hydrolysis was observed in example **5**. Likewise, hydrolysis of the ester group in **6** was not observed, notwithstanding the basic aqueous conditions involved. While substrate **7** containing a quinoline fragment could potentially bind with the NP catalyst and adversely affect the reaction outcome,[25] excellent

selectivity was obtained. Pyrene-containing enone **11** also potentially affecting the selectivity due to possible metal-π interactions did not alter the outcome. No aldol-type side reaction was seen leading to **13**. Likewise, reduction of a formyl group was not observed upon formation of **17**.

Table 2. Substrate scope for selective reduction of enones[a]

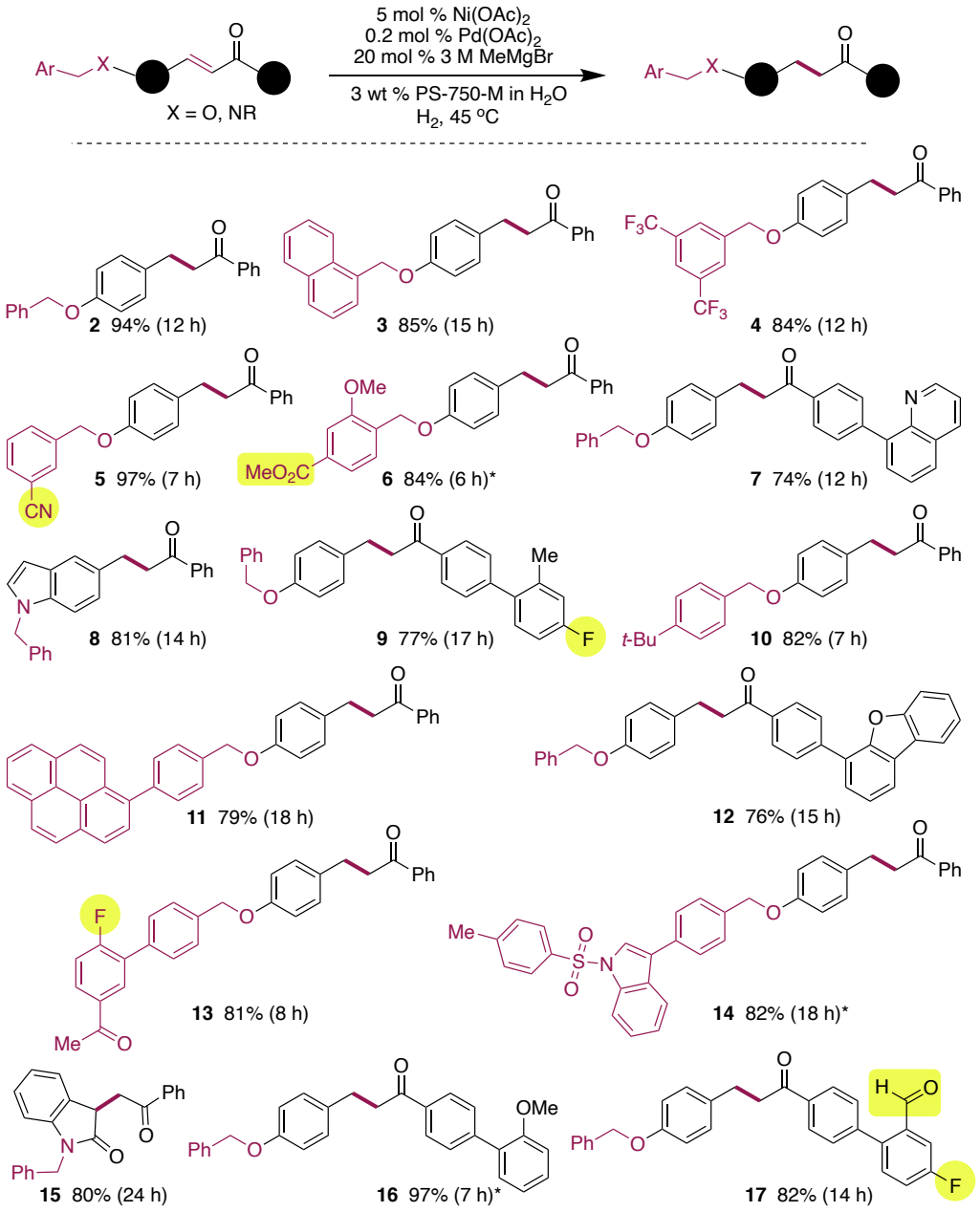

[a]**Conditions**: (i) $Ni(OAc)_2$ (5 mol %), $Pd(OAc)_2$ (0.2 mol %), THF (0.5 mL), 60 °C, 5 min; (ii) 3 M MeMgBr (20 mol %), rt, 5 min; (iii) 3 wt % aq. PS-750-M (1.5 mL), enone (0.5 mmol), H_2, 45 °C. All yields are isolated; *0.25 mmol scale reaction.

Activity tests were further performed to examine the generality in substrates without *N*- or *O*-benzyl groups (Table 3, **18**-**26**). The catalyst was effective for such substrates. Compounds containing heterocyclic residues, such as furanyl (**18**), thiophenyl (**19**), indole (**20**), and pyrazolyl (**26**), readily participated in enone reduction. Notably, an unprotected indole's NH group did not lead to byproduct formation, and compound **20** was cleanly obtained in excellent isolated yield. Sensitive functional groups, such as a silyl ether (**21**) and sulfonate ester (**22**, **26**), were well tolerated. Excellent selectivity was obtained leading to **25** as the major product, where only one double bond of the dienone was selectively reduced; only 10% of the product from double reduction was observed.

Table 3. Activity test on enones containing no *N*- or *O*-benzyl groups[a]

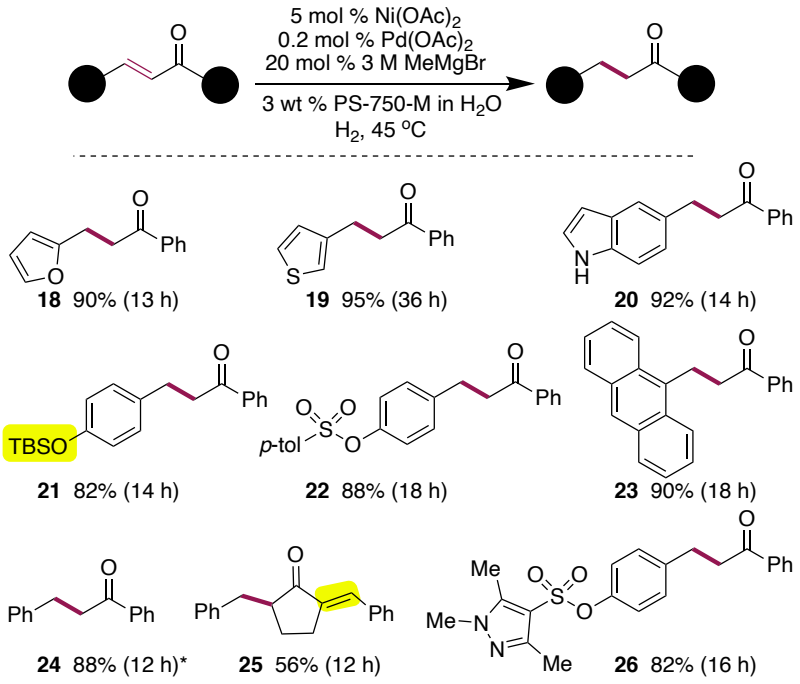

[a]**Conditions**: (i) $Ni(OAc)_2$ (5 mol %), $Pd(OAc)_2$ (0.2 mol %), THF (0.5 mL), 60 °C, 5 min; (ii) 3 M MeMgBr (20 mol %), rt, 5 min; (iii) 3 wt % aq. PS-750-M (1.5 mL), enone (0.5 mmol), H_2, 45 °C. All yields are isolated; *0.25 mmol scale reaction.

The utility of the Ni/Pd bimetallic NPs was further examined involving substrates that are isolobal to enones, such as enenitrile and enamide (Scheme 1a). Clean conversion to **27** was observed without the formation of any polymeric byproducts. Most notably, no nitro group reduction was observed en route to **28**. This technology is also amenable to enamide reduction without intermolecular Michael-type side reactions (**29**), and to selective reduction of α-ketoamide (Scheme 1b). No debenzylation and/or amide reduction were observed for substrate **30**, with only product **31** resulting from 1,4-selective reduction being obtained in excellent yield.

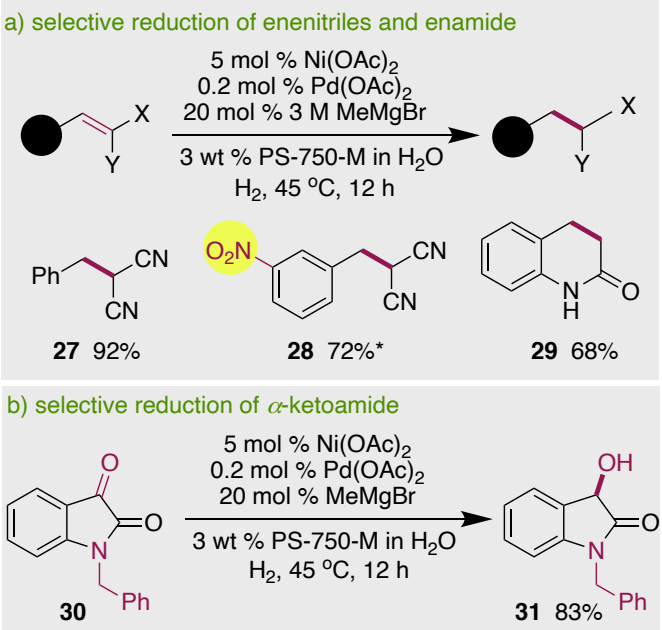

Conditions: (i) $Ni(OAc)_2$ (5 mol %), $Pd(OAc)_2$ (0.2 mol %), THF (0.5 mL), 60 °C, 5 min; (ii) 3 M MeMgBr (20 mol %), rt, 5 min; (iii) 3 wt % aq. PS-750-M (1.5 mL), substrate (0.5 mmol), H_2, 45 °C. All yields are isolated. *0.4 mol % $Pd(OAc)_2$ was used in the catalyst for this example; except 72% isolated desired product, *ca.* 10% byproduct from hydrolysis of enenitrile was observed; no nitro reduction was observed.

Scheme 1. Selective reduction of enenitrile, enamide, and α-ketoamide.

Next, the activity of *in-situ* prepared NPs was compared with that of the isolated catalyst. NPs exposed to air for 24 hours prior to use and state-of-the-art Pd/C catalysts were also tested (Scheme 2A). The activity of the isolated NP catalyst was comparable to the *in-situ* formed NPs, while the

air-exposed catalyst was not selective. With the air-exposed NPs, only 26% of desired product **2** was observed. In comparison, 50% debenzylated byproduct **32** was formed, with the remaining mass being the unidentifiable byproduct observed by GC-MS analysis (for details, see Supplementary Information, page S4). The loss of selectivity is most likely due to the oxidation of Ni in the NPs. Likewise, the Pd/C catalyst was non-selective, and only 44% of desired product **2** was obtained along with **33** (6%) and other unidentifiable byproducts.

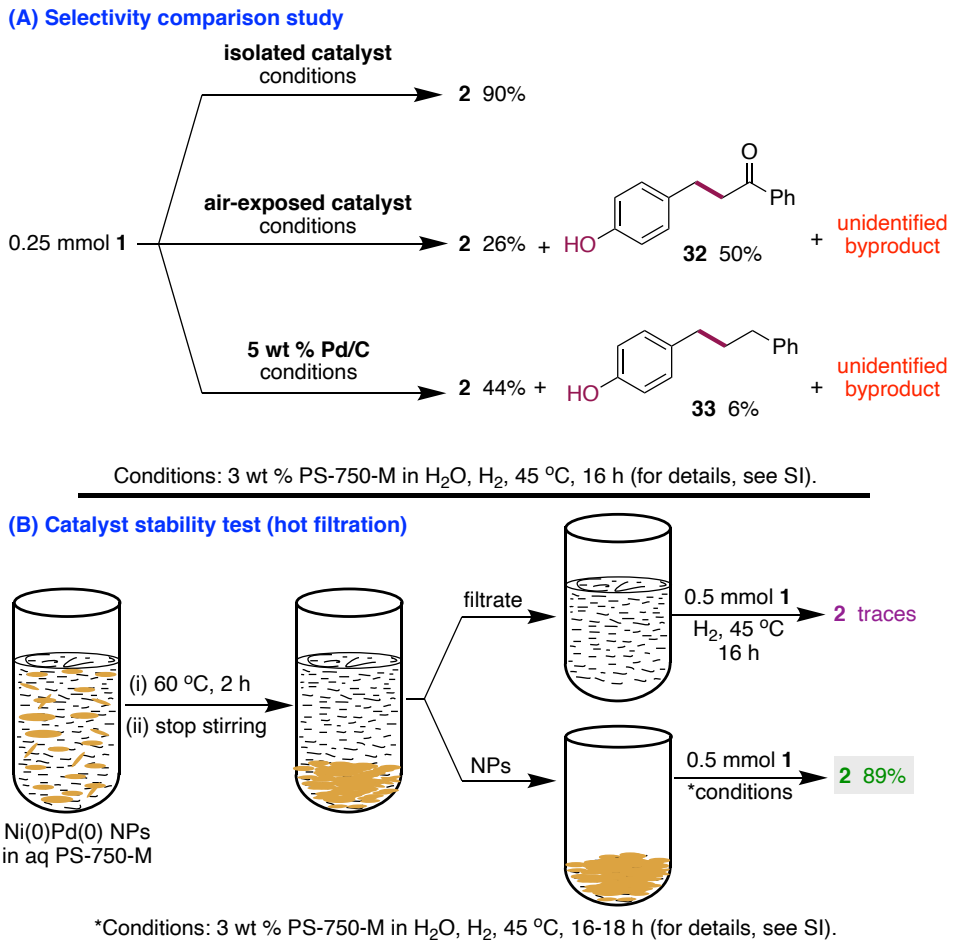

Scheme 2. Selectivity comparison and catalyst stability tests.

Catalyst stability was then tested by hot filtration tests (Scheme 2B, also see Supporting Information). NPs after hot filtration were highly active, leading to the formation of **2** in 89%

isolated yield. The filtrate solution was also tested for activity, and only traces formation of **2** was observed in thin-layer chromatographic analysis. Notably, when a hot filtration test was performed under air, the catalyst activity was reduced, and only a 63% yield of **2** was achieved. This is most likely due to the oxidation of Ni(0). The filtrate obtained after hot filtration under air was completely inactive. Thus, these results support that the catalyst is stable under an argon atmosphere. The catalyst is non-recyclable due to air-exposure needed for reaction workup.

Raman and surface-enhanced Raman scattering (SERS) spectroscopies were used to provide insight into the binding of PS-750-M with the Ni/Pd NPs (Figure 2). The SERS spectrum of PS-750-M capped Ni/Pd NPs (red curve) shows vibrational modes at 995 cm^{-1} and 1476 cm^{-1} that match well to vibrational modes at 989 cm^{-1} and 1478 cm^{-1} of the neat PS-750-M (black curve). This observation indicates the amphiphile's presence in both samples. The amide carbonyl vibrational mode at 1624 cm^{-1} in the neat PS-750-M shifts to 1611 cm^{-1} in Ni/Pd NPs. The 13 cm^{-1} shift to a lower wavenumber implies that the amide carbonyl is physisorbed to the metal surface. Likewise, the ester carbonyl vibrational mode is measured at 1773 cm^{-1} in the neat PS-750-M, while it appears as a shoulder at 1757 cm^{-1} in Ni/Pd NPs. This frequency shift indicates that the ester carbonyl is physisorbed onto the metal NPs. Furthermore, the new vibrational modes at 1999 cm^{-1}, 1317 cm^{-1}, and 1260 cm^{-1} observed in Ni/Pd NPs do not match the neat PS-750-M SERS spectrum or the Raman spectra of the precursor salts (Figure 2, blue and green curves). The shifts in vibrational modes and appearance of new vibrational modes are strong evidence of metal-amphiphile binding, which is potentially responsible for catalyst selectivity.

To gain further insights into the catalyst, Ni/Pd NPs in PS-750-M were characterized by optical microscopy (for details, see Supporting Information, S20-S23). Figures 3A-B show representative optical images of the Ni/Pd NPs in PS-750-M. The images reveal the formation of vesicles

accommodating Ni/Pd NPs either inside the micellar cavity or at the interface. Analysis of *ca*. 100 vesicles indicate an average diameter of 2.4 ± 0.2 μm (Figure 3C). With a coefficient of variation of 0.08, the vesicles are highly monodispersed. Additional optical images also show aggregation of the individual vesicles, which is most likely due to the drying process used in the analysis (for details, see Supporting Information, page S21).

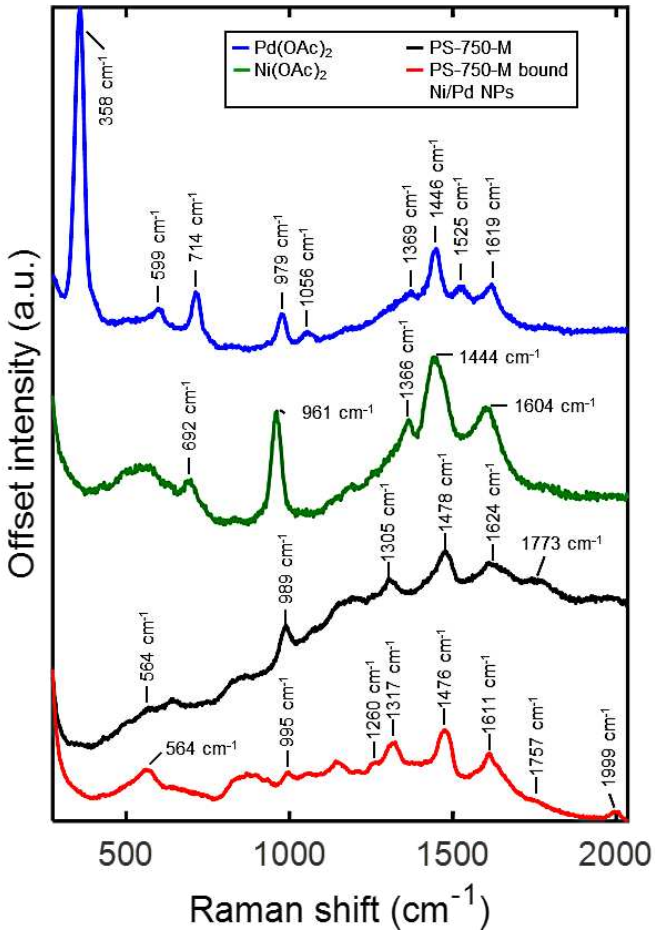

Figure 2. Raman and SERS spectra of the PS-750-M capped Ni/Pd nanoparticle catalyst and the individual components that make up the catalysts. Raman spectra of $Pd(OAc)_2$ and $Ni(OAc)_2$ precursor salt crystals are shown by the blue and green curves, respectively. SERS spectra of PS-750-M with and without Ni/Pd nanoparticles are shown by the red and black curves, respectively. All samples were mounted on a roughened Ag electrode and spectra were acquired with 532 nm laser excitation.

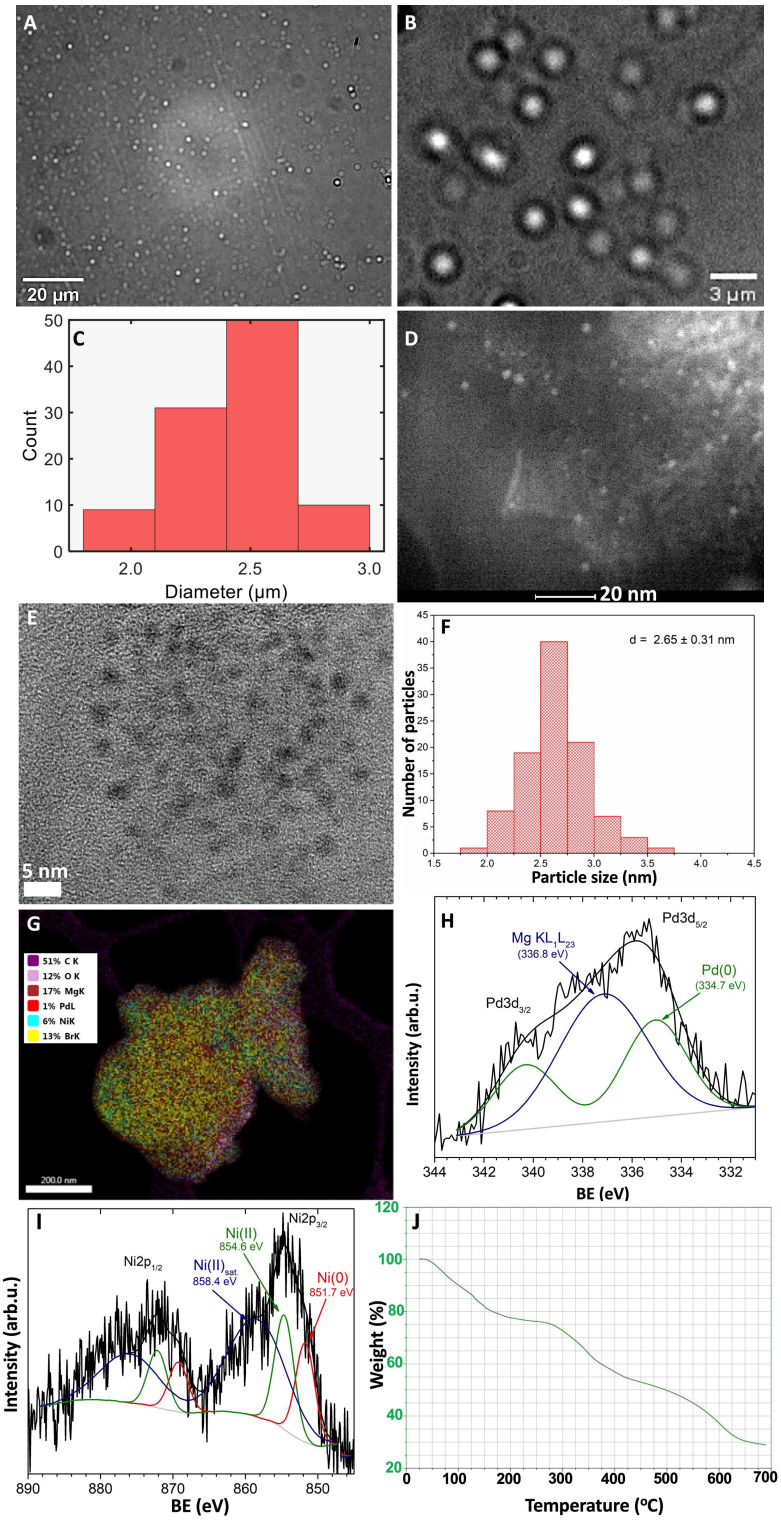

Figure 3. Physical and chemical analysis of Ni/Pd bimetallic nanoparticles. (A, B) Optical microscopy images showing nanoparticles encapsulated by micelles. (C) Histogram showing size distribution of micelle-encapsulated nanoparticles. (D) Scanning transmission electron microscopy-high-angle annular dark-field imaging (STEM–HAADF). (E) High-resolution transmission electron microscopy (HRTEM)

imaging. (F) Histogram showing size distribution of nanoparticles. (G) Energy Dispersive X-Ray Analysis (EDAX) analysis; (H, I) X-ray photoelectron spectroscopy (XPS) analysis. (J) Thermogravimetric analysis.

Scanning transmission electron microscopy-high-angle annular dark-field imaging (STEM–HAADF) reveals the NP nature of the actual catalyst (Figure 3D). However, these particles tend to aggregate easily under high-energy electron beams, limiting STEM–HAADF imaging acquisition. To further study the distribution, morphology, and size of Ni/Pd NPs, high-resolution transmission electron microscopy (HRTEM) analysis was conducted. HRTEM imaging indicated the formation of uniform ultrasmall Ni/Pd NPs with an average size of 2.65 nm (Figure 3E, F). EDX mapping reveals the presence of carbon and oxygen or nitrogen from the amphiphile and Pd and Ni from the bimetallic NPs (Figure 3G). The higher amount of Pd in EDX analysis than the actual amount used NP preparation is most likely due to more Pd on the surface compared to bulk. These combined studies support the formation of ultrasmall bimetallic Ni/Pd NPs located in the micellar interior or interface.

Further, the XPS analysis of the anhydrous NPs confirms the presence of both the Pd(0) and Ni(0). (Figure 3H, I; also see Supporting Information page S18-S19). The presence of peak from oxidized Ni is most likely due to the aerobic oxidation of surfaces during the drying process. The survey spectrum confirmed the presence of Mg, Ni, O, Pd, C (Fig. S5). The peak deconvolution of the Pd3d region yielded a $MgKL_1L_{23}$ and Pd(0) doublet peak, with its $Pd3d_{5/2}$ component at the BE of 334.7 eV.[26] The deconvolution of Ni2p spectrum revealed the Ni(0) at 851.7 eV. Notably, the catalyst was air-sensitive and due to air exposure, Ni(II) was also observed in the analyte. Ni(II) doublet line with its $Ni2p_{3/2}$ component at 856.6 eV and the Ni(II) satellite doublet line with its $Ni2p_{3/2}$ component at 858.4 eV were detected.[27] The deconvolution of the O1s peak produced one strong line at 531.5 eV and two weaker ones, at 530.0 and 533.1 eV, respectively.[28] The peak

analysis of the C1s spectrum, yielded a strong line at 284.5 eV and two weaker lines at 282.8 and 285.8 eV, respectively.[29]

Thermogravimetric (TGA) analysis reveals that the catalyst is stable at elevated temperatures of 180 °C (Figure 3J). A slight loss of weight from 60-180 °C is most likely due to the loss of magnesium-bound THF used in catalyst preparation. A gradual loss of mass after 200 °C may be due to the loss of hydrocarbons from the amphiphile PS-750-M. Based on TGA analysis, the catalyst can be used above 60 °C, if needed, or stored at elevated temperature under an inert atmosphere.

Lastly, the scalability of this technology was also evaluated on a gram-scale reaction. Substrate **1** was exposed to selective catalysis using the optimized conditions to obtain product **2** in excellent yield (see Supporting Information, page 15).

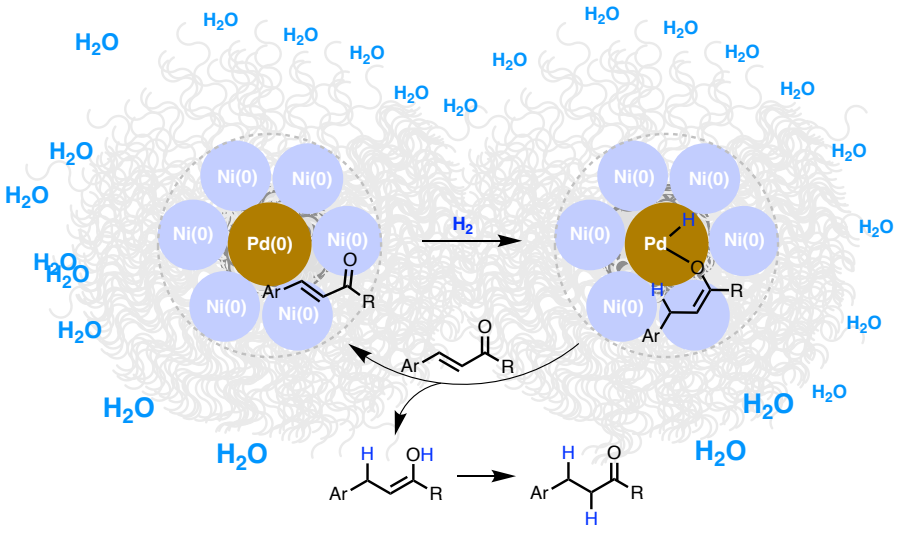

Scheme 3. Plausible reaction mechanism.

Based on the combined experimental findings, a plausible reaction mechanism is depicted in Scheme 3. Most likely, the active catalyst is composed of Ni(0)Pd(0). The presence of Ni(0) around

Pd(0) is potentially responsible for catalyst selectivity. Ni(0) likely activates the carbonyl of substrates, while Pd(0) causes oxidative addition of dihydrogen. The Ni(0)-bound substrate further reacts with Pd-H, forming the Pd-enolate complex. The resulting species finally releases the desired enol after reductive elimination, with the regeneration of the active catalyst. The enol gets converted into a more stable corresponding *keto* product.

Conclusion

In summary, new Ni(0)Pd(0) bimetallic NPs in an aqueous micellar medium are easily prepared that catalyze 1,4-reductions of a variety of Michael acceptors and related substrates. They offer a highly selective protocol that tolerates typically removable protecting groups. Micelles of PS-750-M play a crucial role, enabling the reaction's selectivity, as the desired transformation does not proceed in an aqueous medium containing mPEG or proline. NPs without Ni show far lower activity, and can lead to byproduct formation. In the catalyst, the presence of Pd and Ni in their zero oxidation states is critical for achieving reactions selectivity. This bimetallic catalyst, when compared to Cu-H, avoids competing 1,2-reduction, and uses only hydrogen as a reductant rather than waste-generating hydrosilanes. Interestingly, since these bimetallic NPs are under the influence of the non-racemic environment of PS-750-M, the potential for asymmetric reductions in water without reliance on non-racemic phosphine or other related ligands is especially exciting. Such findings from these laboratories will be described in due course.

ASSOCIATED CONTENT

Supporting Information. Materials and methods, Supplementary Figures, Supplementary Tables, Supplementary Schemes, and Analytical Data (file type PDF).

AUTHOR INFORMATION

Corresponding Author

*Sachin Handa – 2320 S. Brook Street, Department of Chemistry, University of Louisville, Louisville, Kentucky 40292, United States. Email: sachin.handa@louisville.edu

Author Contributions

The manuscript was written through contributions of all authors. All authors have given approval to the final version of the manuscript. ‡These authors (DO and PPB) contributed equally.

Funding Sources

This research was supported in part by the National Science Foundation under award number CHE-2044778.

Notes

Authors declare no conflicts to declare.

Acknowledgement

We thank Dr. Dali Qian from the University of Kentucky for assistance in XPS analysis.

REFERENCES

(1) Nabaho, D.; Niemantsverdriet, J. W.; Claeys, M.; Van Steen, E. Hydrogen Spillover in the Fischer-Tropsch Synthesis: An Analysis of Platinum as a Promoter for Cobalt-Alumina Catalysts. *Catal. Today* **2016,** *261*, 17–27.

(2) Favier, I.; Pla, D.; Gomez, M. Palladium Nanoparticles in Polyols: Synthesis, Catalytic Couplings, and Hydrogenations. *Chem Rev*. **2020**, *120*, 1146–1183.

(3) Pham, V. H.; Dang, T. T.; Singh, K.; Hur, S. H.; Shin, E. W.; Kim, J. S.; Lee, M. A.; Baeck, S. H.; Chung, J. S. A Catalytic and Efficient Route for Reduction of Graphene Oxide by Hydrogen Spillover. *J. Mater. Chem.* **2013,** *1*, 1070–1077.

(4) Yabe, Y.; Sawama, Y.; Monguchi, Y.; Sajiki, H. New aspect of chemoselective hydrogenation utilizing heterogeneous palladium catalysts supported by nitrogen- and oxygen-containing macromolecules. *Catal. Sci. Technol.* **2014**, *4*, 260–271.

(5) Ding, Z-C.; Li, C-Y.; Chen, J-J.; Zeng, J-H.; Tang, H-T.; Ding, Y-J.; Zhan, Z-P. Palladium/Phosphorus-Doped Porous Organic Polymer as Recyclable Chemoselective and Efficient Hydrogenation Catalyst under Ambient Conditions *Adv. Synth. Catal.* **2017,** *359,* 2280–2287.

(6) Mahdaly, M. A.; Zhu, J. S.; Nguyen, V.; Shon, Y-S. Colloidal Palladium Nanoparticles for Selective Hydrogenation of Styrene Derivatives with Reactive Functional Groups. *ACS Omega,* **2019,** *4,* 20819-20828.

(7) Felpin, F. X.; Fouquet, E. A Useful, Reliable and Safer Protocol for Hydrogenation and the Hydrogenolysis of o-benzyl groups: The in Situ Preparation of an Active Pd0/C catalyst with Well-Defined Properties. *Chem. Eur. J.* **2010,** *16*, 12440–12445.

(8) Pogorelić, I.; Filipan-Litvić, M.; Merkaš, S.; Ljubić, G.; Cepanec, I.; Litvić, M. Rapid, Efficient and Selective Reduction of Aromatic Nitro Compounds with Sodium Borohydride and Raney Nickel. *J. Mol. Catal. Chem.* **2007,** *274*, 202–207.

(9) Feng, J.; Handa, S.; Gallou, F.; Lipshutz, B. H. Safe and Selective Nitro Group Reductions Catalyzed by Sustainable and Recyclable Fe/Ppm Pd Nanoparticles in Water at Room Temperature. *Angew. Chem., Int. Ed.* **2016,** *55*, 8979–8983.

(10) Pang, H.; Gallou, F.; Sohn, H.; Camacho-Bunquin, J.; Delferro. M.; Lipshutz, B. H. Synergistic effects in Fe nanoparticles doped with ppm levels of (Pd + Ni). A new catalyst for sustainable nitro group reductions. *Green Chem.* **2018,** *20*, 130–135.

(11) Sergeev, A. G.; Webb, J. D.; Hartwig, J. F. A Heterogeneous Nickel Catalyst for the Hydrogenolysis of Aryl Ethers without Arene Hydrogenation. *J. Am. Chem. Soc.* **2012,** *134*, 20226–20229.

(12) Bihani, M.; Bora, P. P.; Nachtegaal, M.; Jasinski, J. B.; Plummer, S.; Gallou, F.; Handa, S. Microballs Containing Ni(0)Pd(0) Nanoparticles for Highly Selective Micellar Catalysis in Water. *ACS Catal.* **2019,** *9*, 7520–7526.

(13) Papageorgiou, E. A.; Gaunt, M. J.; Yu, J. Q.; Spencer, J. B. Selective Hydrogenolysis of Novel Benzyl Carbamate Protecting Groups. *Org. Lett.* **2000,** *2*, 1049–1051.

(14) Weidauer, M.; Irran, E.; Someya, C. I.; Haberberger, M.; Enthaler, S. Nickel-Catalyzed Hydrodehalogenation of Aryl Halides. *J. Organomet. Chem.* **2013,** *729*, 53–59.

(15) Chen, J.; Zhang, Y.; Yang, L.; Zhang, X.; Liu, J.; Li, L.; Zhang, H. A Practical Palladium Catalyzed Dehalogenation of Aryl Halides and α-Haloketones. *Tetrahedron* **2007,** *63*, 4266–4270.

(16) Schäfer, C.; Ellstrom, C. J.; Cho, H.; Török, B. Pd/C-Al-Water Facilitated Selective Reduction of a Broad Variety of Functional Groups. *Green Chem.* **2017,** *19*, 1230–1234.

(17) Wang, S.; Zhou, P.; Jiang, L.; Zhang, Z.; Deng, K.; Zhang, Y.; Zhao, Y.; Li, J.; Bottle, S.; Zhu, H. Selective Deoxygenation of Carbonyl Groups at Room Temperature and Atmospheric Hydrogen Pressure over Nitrogen-Doped Carbon Supported Pd Catalyst. *J. Catal.* **2018,** *368,* 207–216.

(18) Yang, P.; Lim, L. H.; Chuanprasit, P.; Hirao, H.; Zhou, J. S. Nickel-Catalyzed Enantioselective Reductive Amination of Ketones with Both Arylamines and Benzhydrazide. *Angew. Chem., Int. Ed.* **2016,** *55*, 12083–12087.

(19) Murugesan, K.; Beller, M.; Jagadeesh, R. V. Reusable Nickel Nanoparticles-Catalyzed Reductive Amination for Selective Synthesis of Primary Amines. *Angew. Chem., Int. Ed.* **2019,** *131*, 5118–5122.

(20) Montgomery, J. Nickel-Catalyzed Reductive Cyclizations and Couplings. *Angew. Chem., Int. Ed.* **2004,** *43*, 3890–3908.

(21) Johnstone, R. A. W.; Wilby, A. H.; Entwistle, I. D. Heterogeneous Catalytic Transfer Hydrogenation and Its Relation to Other Methods for Reduction of Organic Compounds. *Chem. Rev.* **1985,** *85*, 129–170.

(22) Handa, S.; Wang, Y.; Gallou, F.; Lipshutz, B. H. Sustainable Fe–ppm Pd nanoparticle catalysis of Suzuki-Miyaura cross-couplings in water. *Science* **2015**, *349*, 1087–1091.

(23) Plieth, W. J. Electrochemical Properties of Small Clusters of Metal Atoms and Their Role in Surface Enhanced Raman Scattering. *J. Phys. Chem.* **1982,** *86* 3166–3170.

(24) Pattadar, D. K.; Zamborini, F. P. Size Stability Study of Catalytically Active Sub-2 Nm Diameter Gold Nanoparticles Synthesized with Weak Stabilizers. *J. Am. Chem. Soc.* **2018,** *140*, 14126–14133.

(25) Handa, S.; Ibrahim, F.; Ansari, T. N.; Gallou, F. π-Allylpalladium Species in Micelles of FI-750-M for Sustainable and General Suzuki-Miyaura Couplings of Unactivated Quinoline Systems in Water. *ChemCatChem* **2018,** *10*, 4229–4233.

(26) Li, Y.; He, Y. Layer Reduction Method for Fabricating Pd-coated Ni Foams as High-performance Ethanol Electrode for Anion-exchange Membrane Fuel Cells. *RSC Adv.* **2014,** *4*, 16879-16884.

(27) Grosvenor, A. P.; Biesinger, M. C.; Smart, R. St. C.; McIntyre, N. S. New interpretations of XPS spectra of Nickel Metal and Oxides. *Surf. Sci.* **2006,** *600*, 1771–1779.

(28) Krishnan, P.; Liu, M.; Itty, P. A.; Liu, Z.; Rheinheimer, V.; Zhang, M.-H.; Monteiro, P.J. M.; Yu, L. E. Characterization of Photocatalytic TiO2 Powder under Varied Environments using Near Ambient Pressure X-ray Photoelectron Spectroscopy. *Sci. Rep.* **2017,** *7*, 43298.

(29) Moulder, J. F.; Stickle, W. F.; Sobol, P. E.; Bomben, K. D. *Handbook of X-ray Photoelectron Spectroscopy*; Chastain, J. Eds.; Perkin-Elmer Corporation; **1992.** ISBN: 0962702625.

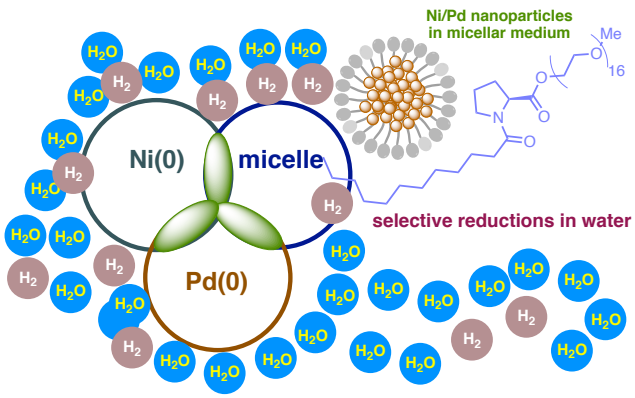

Ni/Pd bimetallic nanoparticles in aqueous micellar medium leads selectivity toward 1,4-reductions in the presence of sensitive benzyl, nitro, aldehyde, and other functional groups—in water reaction offers safe handling of flammable hydrogen gas as clean hydride source.